Scientific original paper

Informacije MIDEM
Journal of Microelectronics,
Electronic Components and Materials
Vol. 42, No. 3 (2012), 164 – 175

Microfabrication and characterization of microcombustor on (100) silicon /glass platform

D. Resnik[1,2], S. Hočevar[3,4], M. Možek[1,2], I. Stegel[5], S. Amon[1,2] and D. Vrtačnik[1,2]

[1]*University of Ljubljana, Faculty of Electrical Engineering, Laboratory of Microsensor Structures and Electronics,*
[2]*Centre of Excellence Namaste, Jamova 39, Ljubljana 1000, Slovenia*
[3]*National Institute of Chemistry, Laboratory of Catalysis and Chemical Reaction Engineering, Hajdrihova 19, SI-1000 Ljubljana, Slovenia*
[4]*Centre of Excellence for Low Carbon Technologies (CoE LCT), Hajdrihova 19, SI-1000 Ljubljana, Slovenia*
[5]*Ministry of Defense of the Republic of Slovenia,*

Abstract: Design, microfabrication process steps and characterization of catalytic microcombustors built on (100) silicon-glass platform are presented. Investigation of catalytic combustion regimes for three distinct energents (H2+O2, methanol+O2, methanol+air), fed into the combusting microcavity via pre-mixing through the bubbler or via in-situ mixing on the platform was carried out. Thermodynamic properties, dependent on ignition parameters, light–off temperature and thermal response for various input flow conditions in the temperature range between 80-320 °C were investigated and the results are discussed. It was determined that two-phase flow in microchannels can cause significant pressure oscillations which may degrade the performance of the microcombustor under certain feed conditions. Catalytic combusting via thin film nanodispersed Pt/CeO2 catalyst proved very efficient, showing light- off for combusting H2-O2 already at room temperature and in case of methanol-air combusting reagents at 80 °C. Under optimal conditions, assembled microcombustor was able to provide continuously 4.6 W thermal power, reaching the temperature of 290 ±1 °C, with 1.1 ml/h consumption of liquid methanol.

Key words: Si-glass micromachining, methanol catalytic combustion, light-off temperature, thermal response

Karakterizacija mikrogorilnika izdelanega na Si (100)/Pyrex steklo podlagi

Povzetek: Predstavljeni so načrtovanje, tehnološki procesi mikroobdelave (100) silicija in stekla ter karakterizacijski postopki za ovrednotenje delovanja mikrosežigalnika. Raziskani so bili pogoji uvajanja in gorenja treh različnih vstopnih energentov (H2+O2, metanol+O2, metanol+air) preko tankoplastnega Pt/CeO2 katalizatorja. Prikazani so vplivi posameznih parametrov (pretoki, razmerja pretokov, tlaki, temperature) na delovanje in odzivnost mikrogorilnika. Raziskali smo možnosti dveh različnih načinov uvajanja energentov in določili ustrezen nabor parametrov za delovanje mikrogorilnika. Prikazana sta primera uvajanja energentov s predmešanjem metanola in kisika/zraka ter uvajanjem ločenih energentov in mešanje na sami platformi. V slednjem načinu doziranja energentov je bil opazen močan vpliv dvofaznega toka tekočinskega toka kot posledica uparjanja metanola v mikrokanalih pred vstopom v katalitsko izgorevalno komoro. Z uporabo nanodispergirane platine na mezoporozni cerijevi podlagi kot katalizatorja smo dosegli vžig H2-O2 energentov že pri sobni temperature, vžig metanola in zraka pa pri temperature 80 °C. Pri optimalnih pogojih smo dosegli stabilno in kontinuirano delovanje načrtanega in izdelanega mikrogorilnika pri temperaturah tudi do 290 ±1 °C ob izredno nizki porabi tekočega metanola 1.1 ml/h.

Ključne besede: mikroobdelava, Si-steklo podlage, katalitsko gorenje metanola, vžigna temperature, termični odziv

1. Introduction

Electronic portable applications require extended period of power supply autonomy. Battery technology can not always satisfy the power demands for the portable electronics [1]. One of the advanced approaches to overcome this problem is the application of proton exchange membrane fuel cells (PEMFC) cells as a port-

---

** Corresponding Author's e-mail: Drago.Resnik@fe.uni-lj.si* able power source [2, 3]. As the input energent, PEMFC require high purity supply of hydrogen. Hydrogen rich gas can be generated from liquid fuel such as gasoline or methanol-water usually by steam reforming (SR) process. In many cases methanol (MetOH) is preferred since it can be efficiently converted into hydrogen at moderate temperatures (<300 °C). Methanol has high H:C (4:1) ratio and no C-C bonds, what minimizes the risk of soot formation which degrades the catalyst performance [4].

The hydrogen fuel processor shown in Fig.1 comprises usually several units in series: evaporizer for methanol-water input energent, SR unit, and preferential oxidation (PrOx) unit. PrOx unit is used to clean-up the hydrogen rich stream by reducing CO amount below e.g. 50 ppm range since higher amount of CO can be poisonous for proton exchange membrane and consequently for fuel cell operation. In certain cases when CO content is too high, water-gas-shift unit (WGS) is included between the SR and PrOx unit. The steam reforming is an endothermic process. Therefore, energy must be provided on board for both, evaporation of fuel and SR reaction. For this purpose methanol combustor can be used as an appropriate indirect heat source, providing heat to support and maintain the required reactions taking place in fuel processor. This is typically attained by burning a small amount of hydrocarbon fuel. Microcombustors as heat providers are also met in other applications such as in thermophotovoltaic power generators [5] or thermoelectric devices [1, 6].

The leading idea in our case is to utilize the same fuel source (MetOH) for both, SR and catalytic combusting. In the case of excess production of H_2 from SR unit or unexploited H_2 from FC, the methanol is replaced partially or fully with H_2 to maintain catalytic reaction and providing required heat as indicated in Fig. 1.

In the following paper a detailed investigation of a microcombustor unit is carried out. Catalytic (flameless) combustion is taking place in the combusting chamber over the catalyst layer with specific properties. Combusting thermodynamic process in the presence of catalyst is dependent strongly on contact or residence time and activity of catalyst itself. Different types of catalyst and the support material are met in the literature, such as Pt/ZrO_2 [7], $Pt\text{-}Sn/Al_2O_3$ [8], Pt/TiO_2 [9], Pt/Al_2O_3 [1, 10, 11] Pt/CNT [12]. Heterogeneous catalysts are not sufficiently active at room temperature and require external heat for ignition of the fuel [13]. This preheating is a drawback since it requires additional source of energy. A method to achieve spontaneous self-ignition and self-supporting combustion of premixed methanol-air at room temperature (RT) with nanosized Pt catalytic particles has been reported by Ma et al. [14] for glass tube reactors. Nanosized catalytic particles are significantly more reactive than their bulk counterparts, exhibit high specific surface areas and can significantly increase the performance of catalytic combustors. In this work, developed nanodispersed Pt catalyst on mesoporous CeO_2 support was applied with specific surface areas exceeding 130 m^2/g providing even RT ignition in the case of H_2+O_2 combusting.

The main objectives of the presented study were to develop a catalytic microcombustor with Pt/CeO_2 catalyst and to evaluate its thermal performance, with respect to various input energents (H_2+O_2, MetOH+O_2, MetOH +air), their flow ratio and flow rates. For this purpose, a Si platform with microchannels, mixers and combusting cavity were designed, fabricated and hermetically sealed by Pyrex 7740 glass with anodic bonding technique to provide fluid connections between the pump and microchannels. Besides, advanced DRIE silicon bulk micromachining and newly developed thin film deposition technique for catalyst layer were applied to realize functional microcombustor microfluidic system.

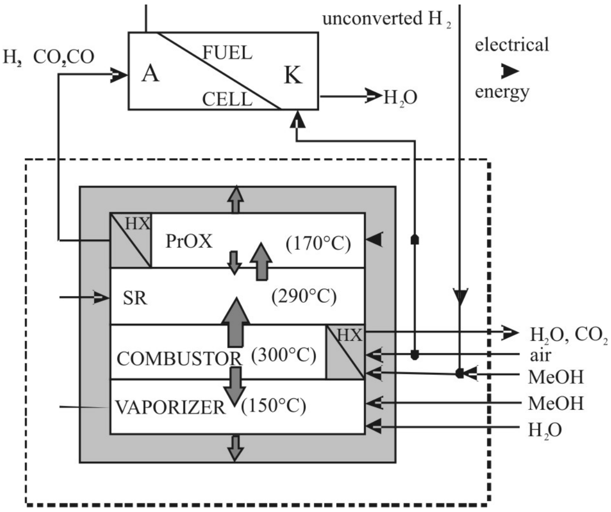

Figure 1: Conceptual integration of components and heat flow in methanol-to-hydrogen fuel processor for PEMFC.

2. Experimental work

Microfabrication process

Basic fabrication steps are presented in Fig. 2. Silicon microfabrication was performed on low resistivity (10-15 Ωcm), n-type, single side mechanically polished float zone (FZ) silicon wafers with {100} crystal orientation.

The masking layer during etching was a 9 µm thick film of AZ 9562 photoresist (Fig.2a). Etching of microchannels and cavity in Si (Fig.2b) was performed by deep reactive ion etching (DRIE) process in Plasmalab 80 etcher. The depth of input channels and cavity was 140 µm and width of the inlet channels was 600 µm. After performing DRIE process, the resist was removed in the oxygen plasma reactor Tegal 412 and the wafers were diced into individual Si platforms (35x27 mm^2) and deposition of Pt/CeO$_2$ catalyst was performed. The Pt (2.0 wt.%)/CeO$_2$ catalyst precursor was prepared as described elsewhere [15, 16].

A special technique of depositing thinner films in several consecutive depositions was applied to avoid the catalyst film cracking problems. It was determined experimentally that the deposition of a single, thick film has to be avoided due to the cracking of the film, which is later usually peeled off after drying or after calcinations. As the last step, the calcination of cumulative catalyst layer was performed in air ambient at 600 °C for 10 hours (Fig. 2c).

The quantity of Pt catalyst in the cavity was determined after the calcination and was 4 and 7 mg (balance Kern ABJ120-4MJ with 0.1 mg resolution) for depositing three or five layers, respectively. Thickness measurements of catalysts layer were performed by depth focus measurements and cross-sectioning revealing a value of 20-30 µm. The cavity area where catalyst was deposited was 360 mm^2.

Cleaning and removal of any particles prior to Si-glass bonding is essential for good hermetic sealing of the cavity, since during several deposition steps of catalyst it is very likely that some slurry is dragged toward the bonding surface, despite the hydrophobic nature of the latter. Prior to the anodic bonding operation, Si and Pyrex surfaces were cleaned thoroughly by 2-propanol and DI water, dried by nitrogen and brought into intimate contact under cleanroom environment.

To observe and characterize the flow behavior and ongoing reactions, a transparent cover made of Pyrex 7740 (Dow Corning) glass, 700 µm thick, anodically bonded onto silicon microchannel platform was provided. To enable fluid connections, Pyrex glass had prefabricated inlet and outlet through holes (Fig. 2d). Through holes in Pyrex glass (diameter 800 µm) were fabricated by micro-drilling technique. A special fixture was developed to align Pyrex and Si platform, to obtain accurate positioning (±10 µm) of through holes of Pyrex and in/out connections of microchannels. Pyrex was then bonded to silicon by anodic bonding at 385 °C and applied anodic voltage of 1000 V (Fig. 2e).

Prior to testing, catalyst treatment in a reduction ambient (H$_2$ at 180 °C for 2 hours) was carried out. After the microreactor was completed the mounting in a packaging case was performed. Stainless steel (SS) (thermal conductivity λ= 17 W/mK @ 25 °C) housing with fluidic connection were designed rigid enough to enable reliable packaging, fast replacement of device under test and hermeticity at working temperature. Explicity, PTFE housing with low thermal conductivity (λ = 0.25 W/mK @ 25 °C) was used for initial tests for H$_2$-O$_2$ combustion experiments only. In Fig. 3 SS case is shown, consisting of two separate parts, top one with laser welded SS tubes for fluidic connections and bottom one with the recessed seat for combustor platform (Fig.3). Rock wool insulation BS15, 25mm thick with thermal conductivity λ = 0.093 W/mK @ 200 °C was used for thermal insulation during tests, unless otherwise mentioned. Inset in Fig. 3 reveals detail of a gas distributor design enabling homogeneous distribution of vaporized input reagents across the entire cavity thus providing uniform temperature.

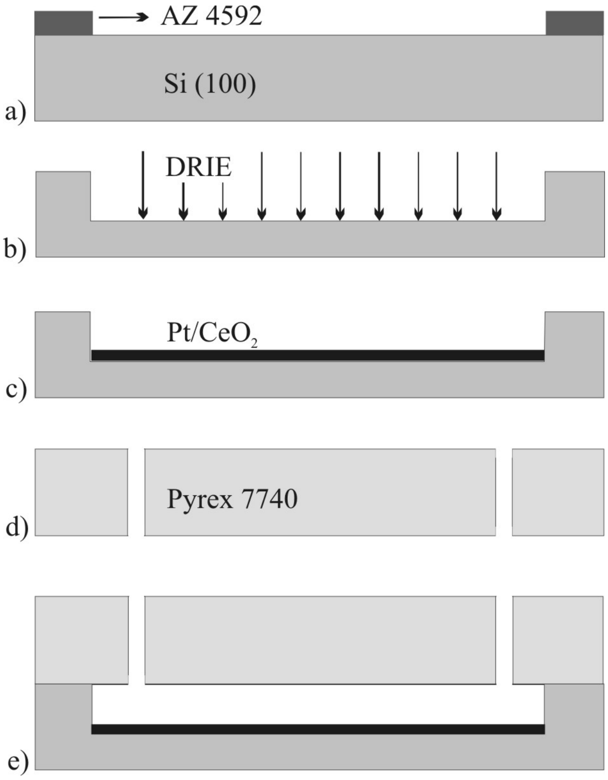

Figure 2: Microcombustor fabrication steps; a) Si microchannel, mixer and cavity patterning, b) DRIE Si deep etching (150 µm), c) deposition of catalyst, d) Pyrex microdrilling and micropositioning of in/out ports, e) aligning and anodic bonding of Si and Pyrex.

Characterization setup

In order to cover a wide range of variables and to maintain good process control of various parameters, the characterization setup was conceived in a modular

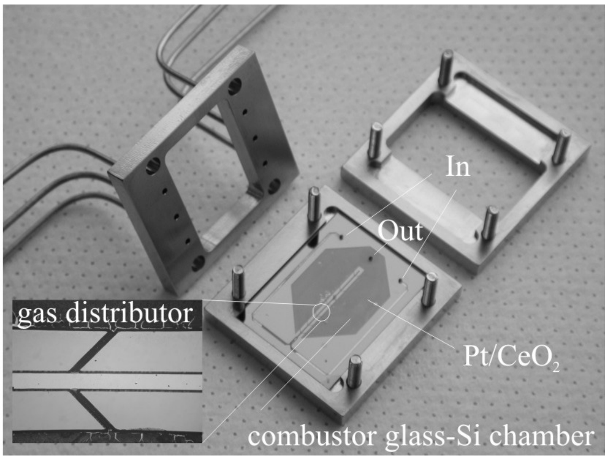

Figure 3: Stainless steel housing with in/out fluid connections and combustor microreactor.

way. This approach enabled fast and reliable multiple measurements with exchangeable combusting platforms and easy switching between different inlet fuel streams.

The temperature measurements were performed by measuring the combustor cover glass temperature and the reactor housing temperature with Pt-100 and K-type temperature sensors, respectively. During experiments the reactor was surrounded by rock wool insulation and the temperature measured on the housing equals to average combustor platform temperature after a certain period. The temperature is a direct indicator of reaction intensity and the measured amount of output water can be taken as a figure of merit and correlated to overall reaction efficiency. The setup also included pressure and flow controllers for the input quantities.

3. Results and discussion

The designed and fabricated microcombusting platforms were characterized with respect to two different types of combusting fuel (H_2+O_2 or MeOH +air/oxygen) and with respect to two different modes of applying MeOH+ air/oxygen fuel, i.e. by two separate inputs and mixing on the platform or by premixing of methanol and air/oxygen in the bubbler and introducing mixed vapor phase via a single input into the combustor. Characterization was performed by the developed setup shown in Fig. 4.

Characterization of combustor with H_2+O_2 energents

In this mode of combusting, separate input microchannels for hydrogen and oxygen were designed and fabricated. Mixing of both gases occurs in the microreactor, just prior to reaching the catalyst zone. The mixers were Y type or nozzle type, the same as used for experiments in subsection 3.2 and 3.3.

Total oxidation i.e. combustion of hydrogen and oxygen via catalyst is described by the following equation:

$$2H_2(g) + O_2(g) = 2H_2O(l) + 286\ kJ/mol\ (HHV) \tag{1}$$

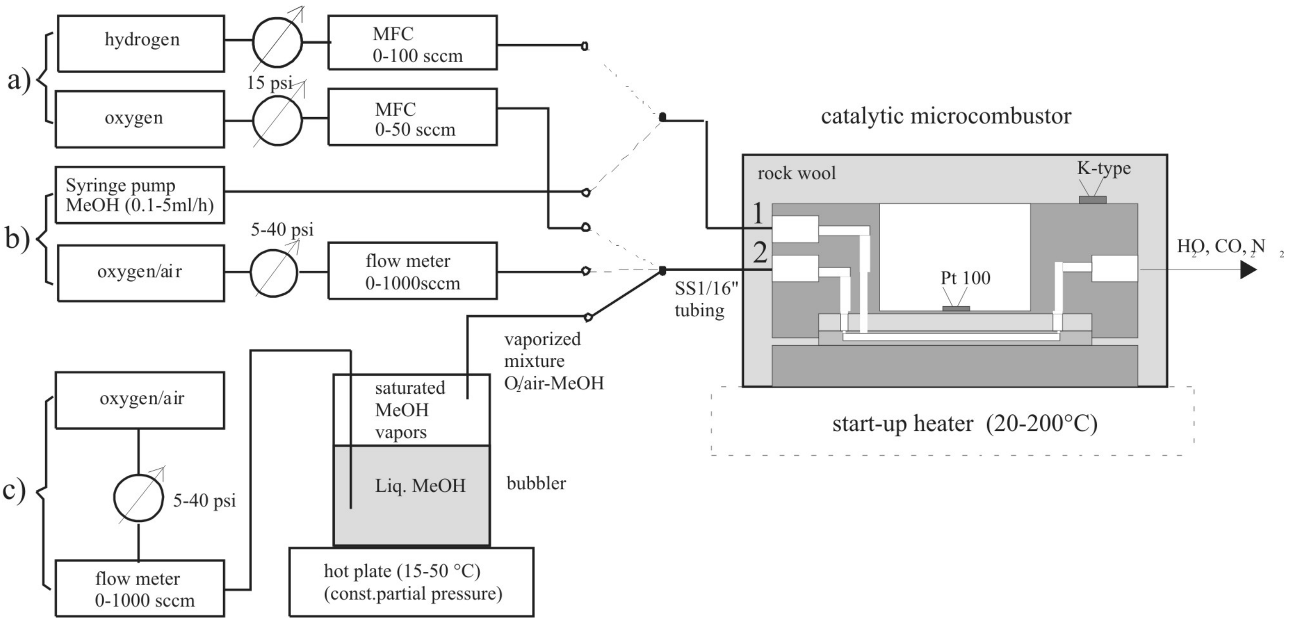

Figure 4: Characterization setup enabling three configurations of input reagents and feed modes: a) combusting of H_2 and O_2, b) combusting of MetOH and O_2/air and c) combusting of premixed MetOH+O_2/air.

where enthalpy of combustion ΔH =286 kJ/mol is the higher heating value (HHV). For the case shown below (Fig. 5), e.g. for inlet flow of O_2=20 sccm and H_2=40sccm, the output of Φ_{H2O}=32 μl/min and calculated heat power of P_{th}= 8.5 W can be obtained in stoichiometry by assuming the 100% efficiency of the combustor.

It is shown in Fig. 5 that the spontaneous ignition for reaction of H_2 and O_2 can take place on the catalyst successfully already at room temperature, however, the amount of water product shows efficiency slightly above 50%. Nevertheless, this is strong evidence that the prepared nanodispersed Pt on mesoporous ceria oxide is highly active and appropriate type of catalyst, since it starts the reaction at such low light-off temperature. The temperature where reaction takes place is called a light-off temperature and is defined as the temperature at which a catalytic converter achieves 50 % conversion rate.

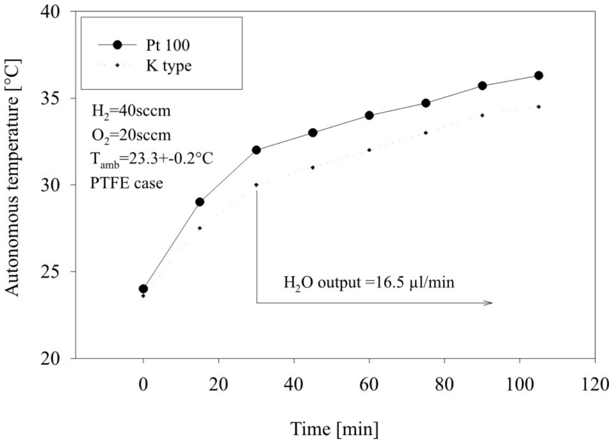

Figure 5: Microcombustor spontaneous ignition obtained at room temperature

Due to high mass load of the combustor PTFE housing (170 g) and slow transition from heterogeneous reaction, the reached final temperature is low, but the reaction is self- sustained. The combusting efficiency in this case was correspondingly low (<50 %) regarding the measured amount of the output water.

By increasing the light-off temperature to 100 °C (Fig. 6), the rise time was decreased and the self-sustained process increased and maintained the temperature of the combustor system at 135 °C and also responded instantly on the increased flow rate of both reagents to new value of 50 and 25 sccm for H_2 and O_2, respectively. The amount of output water was increased compared to RT ignition from 16.5 to 18 μl/min (efficiency 56%). No additional insulation was put around the PTFE housing in this case. Due to PTFE thermal limitation and material softening (loss of rigidity), it was observed that latter can not provide sufficient hermeticity above 180 °C. Therefore, despite having much lower thermal conductivity, PTFE housing was replaced for all further experiments by SS housing as shown in Fig. 3.

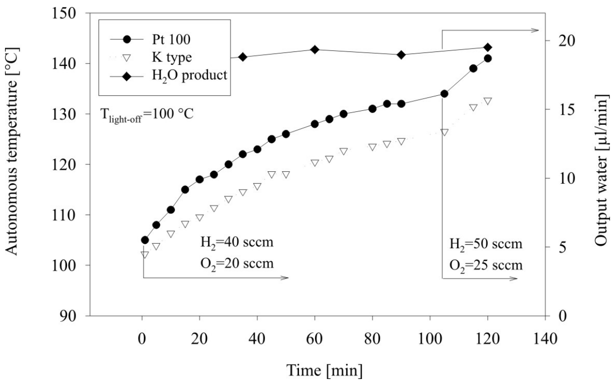

Figure 6: Combustor temperature and amount of output water vs. time for H_2-O_2 reagents at light-off temperature 100 °C (PTFE case)

By designing new, SS housing with smaller outer dimensions and lower mass (100 g) as well as using 20 mm thick rock wool insulation, the temperature rise time (Fig.7) was actually not improved. This is attributed to higher thermal conductivity compared to PTFE. However, with the implemented heat insulation and reduced heat losses, the final temperature reached 205 °C under the same feed conditions, while combusting efficiency increased to 63%. H_2-O_2 experiments were conducted mainly to prove the catalyst reactivity at RT and increased fuel flow rate experiments were not considered further in this study due to limited measuring range of available MFC flow controllers.

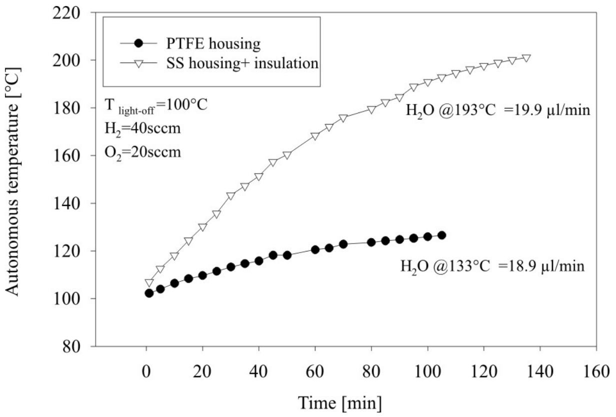

Figure 7: Comparison of the same reactor platform in PTFE and SS housing and with improved isolation, for the same feed conditions.

Estimated error in acquisition of output water was in the range of 10-15%, due to losses of water vapor prior to reaching the cold trap rather than at weighing procedure, so the efficiency is actually higher.

By measuring the quantity of output water, it is shown that at higher start up temperatures, increased amount of output water is obtained, which is closer to theoretical value, meaning that the combusting efficiency is increased.

Since the outlet gas stream from the combustor (water vapor, unreacted gas) is nearly at the temperature of combustor and the condensing heat is delivered to the surrounding after exit, it should be recuperated in a proper way. One way of recuperation is used in our design and consists of placing output near the inlet ports so part of downstream heat is transferred to the cold incoming gas. Another way to recuperate the condensation heat of the exit water vapor to the inlet H_2 and O_2 gas stream is to put in physical contact inlet H_2 and O_2 tubes with exiting hot tube in a manner of counter flow heat exchanger (depicted as HX in Fig.1).

Characterization of combustor with internal mixing of MeOH + O_2

To start the exothermic reaction, certain conditions must be fulfilled: efficient catalyst layer, appropriate dimensions of cavity to stay well below explosion limits and start up temperature for ignition. Methanol-oxygen catalytic ignition requires high activation energy (high energy input is required). After ignition, the reaction proceeds with a higher rate constant and has lower activation energy compared to the one for ignition. Once ignited, the reaction is sustained as long as fuel and oxygen (air) is available in proper ratio and quantity.

According to work of Hu et al. [13], two distinctive combusting regimes are met (two different reaction mechanisms), depending on different fuel ratio, a slower, heterogeneous-only catalytic reaction on the catalyst surface and a faster, mixed reaction regimes that includes both, hetero catalytic reaction on the nano-particle surfaces and a homogeneous combustion of the methanol + air in gas phase above the catalyst surface, supported by radicals. Combusting of methanol in presence of oxygen is described by the following overall reaction:

$$CH_3OH(l) + 3/2O_2(g) = 2H_2O(l) + CO_2(g) + 726\ kJ/mol\ (HHV) \quad (2)$$

where exothermic heat of 726 kJ/mol (higher heat value, HHV), is produced in reaction with oxygen at stoichiometry. Overall, the heat obtained by combustion has to satisfy the following equation if the combustor is used for SR applications:

$$Q_{comb} > [Q_{heat\text{-}up}+Q_{vap}]_{comb} + [Q_{heat\text{-}up}+Q_{vap}]_{SR} + Q_{SR}+Q_{loss} \quad (3)$$

where first part is to heat up and evaporize the methanol for combusting, the second part is to heat up and evaporize the methanol-water mixture SR feed, the third is to cover the enthalpy of SR process and the fourth is to cover mostly the convective losses toward ambient, due to limited thermal insulation.

E.g. for input flow rate of 1ml/h of liquid methanol MeOH and 13.8 sccm of O_2, the output rate of Φ_{H2O}= 14.8 µl/min is obtained in stoichiometry and the heat power produced is 4.97 W_{th}.

Separate input ports and mixing inside the reactor were applied in this type of combusting (Fig. 8c). Two important parameters should be fulfilled for this type of fuel applications: complete evaporation of the liquid methanol and sufficient degree of mixing methanol vapors and oxygen or air before entering the catalytic zone.

The liquid methanol entering hot zone has to vaporize fully before reaching the mixing point, otherwise it can flood the catalyst cavity and extinct the reaction. This can be fulfilled by increased microchannel length to provide sufficiently long path to fully evaporize the liquid methanol and heat up reactant gas, respectively, before they reach the mixing point.

Sufficient mixing is a prerequisite condition prior to introduction of reactants into the catalyst covered combustor cavity. Due to laminar flows in microchannels this is a demanding task, particularly when it has to be performed along a short path. Two approaches were undertaken to support better mixing; one being the introduction of a nozzle to introduce methanol at the point where the reactant gas is added (oxygen or air) and the other is the introduction of mixing obstacles in the microchannel leading toward the combusting cavity (Fig. 8b), similar to [17]. Mixing of two flow streams in microchannels, where usually laminar flow prevail is rather difficult to obtain. The dispersion of solutes occurs by diffusion which is a slow process [17] and in case of geometrically splitting and recombining flow streams with obstacles also by convection in lateral direction. Passive mixing principle was used in our design which does not contribute to pressure drop and also does not introduce any dead volumes [17]. The obstacles, i.e. pillars, were placed asymmetrically in the main microchannel at certain positions, determined preliminary by ANSYS simulating tool (Fig. 8a). The chosen design of mixing pillars also had to comply with the micromachining process for simultaneous fabrication of the whole silicon structure in a single DRIE step and a single mask (Fig. 2b).

Once these conditions are fulfilled, the final temperature (delivered heat energy) of such microcombustor depends on the following parameters: i) input flow of reagents, ii) type, efficiency and quantity of catalyst, iii) thermal isolation, boundary conditions (wall heat transfer) and iv) design issues of microchannels, mixer, cavity and exhaust path (defining pressure drop).

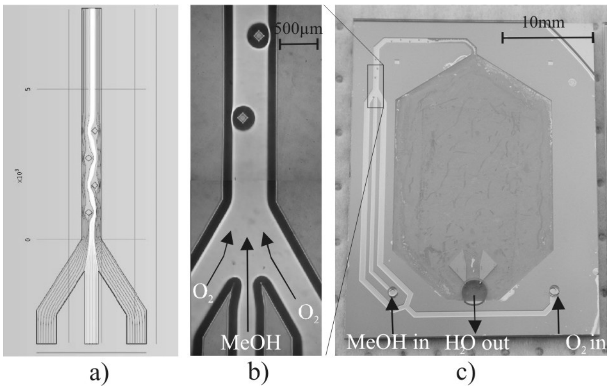

Figure 8: Combustor type1 with designed separate inputs, mixer and micromachined obstructions for improved mixing in the microchannel: a) Ansys modeling, b) top view of a mixer detail, c) completed microcombustor.

In the first set of experiments, performed on microcombustor platforms (mounted into the SS housing and insulated by rock wool) without sufficient mixing efficiency, only insignificant temperature rise was sensed due to the fact that heat losses toward ambient exceeded the generated heat. The only indication that the reaction was taking place was the output water. In certain cases, when mixing was insufficient or fuel rich mixture was applied, the output product was sensed as a mixture of water and unreacted methanol as shown by gas chromatography analyses or with analyzing the contact angle and by comparing it with the reference DI water droplet. Another problem associated with liquid methanol on board evaporation was encountered during experimental work as strong, periodic pressure oscillations.

Pressure oscillations were determined to be a consequence of methanol evaporation process in the microchannel. As observed by Wu et al. [18], this is a common phenomenon for two-phase flow in microchannels. The liquid-vapor interface oscillates as some of the already formed vapor condenses back, causing change of volume and even a reverse flow can be expected in some cases.

In the microcombusting process, similar oscillation of the system was observed as a consequence of the above mentioned phenomenon and/or due to backpressure caused by condensation of water in the exit line. The water product at the exit was observed to be pushed out periodically, when the exit line becomes clogged with the droplet across the pipe diameter. This reflects also on the input feed conditions as a shattering of inlet liquid methanol silicone tube. The coupling of output and input exist via the backpressure oscillations, which may cause the damping and/or extinction of the reaction process in the combusting cavity.

Pressure oscillation during evaporization was also measured in separate experiments for the case of MeOH-DI water (2:1 volumetric) in meandered microchannels, 600 µm wide, 150 µm deep and total length of 150 mm. The pressure oscillations are well observed in Fig. 9, particularly at higher flow rates. The evaporizer was supplied with constant heat power, so the temperature decreased by increasing the amount of input liquid. Besides, as can be seen in illustrations above the graph, the point of fully evaporated liquid moves downstream. The oscillation period was around 60 s for a specific case and the amplitude is increasing by the flow rate of input medium up to 50 mbar at 9 ml/h as shown in the Fig. 9. In this particular case, the electrical heat power of 8.5 W was required to maintain the evaporization and cover heat losses. However, in the presented study of combusting, where the flow rate of liquid methanol never exceeded 1.5 ml/h, the oscillations were of shorter period. Oscillation in pressure is strongly correlated to water droplet formation (condensation) at the exit which in turn influences back the input feed conditions.

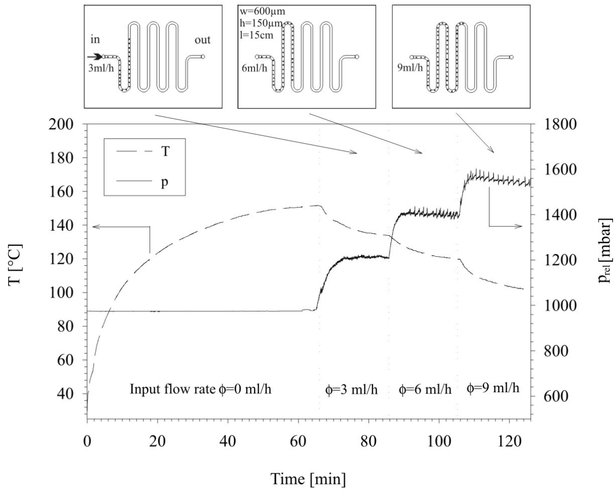

Figure 9: Evaporation of MeOH:DI (2:1vol.) in meandered microchannel: temperature and pressure vs. time for three input flow rates, at constant heating power of 8.5W.

Autonomous combusting for internal mixing of MeOH and oxygen /air was obtained within narrow range of feed parameters. Fig. 10 presents the successful performance of combusting and the obtained temperature in full autonomy once the ignition started at light-off temperature 200 °C (diamond symbols). In the next experiment, the input ports were exchanged. In this case, mixing was presumably improved and higher efficiency as well as higher final temperature (square symbols) was obtained and maintained. Temperature stability in the first case was 200±2 °C in time interval 20-190 min (after which the fuel feed was changed) and 185±3 °C (considering time interval from 15-190 min).

One of the reasons for low increase of temperature in autonomous self-sustained combusting process is that additional heat to evaporize the amount of introduced methanol ($Q_{heat\text{-}up}+Q_{evap}$) must be provided.

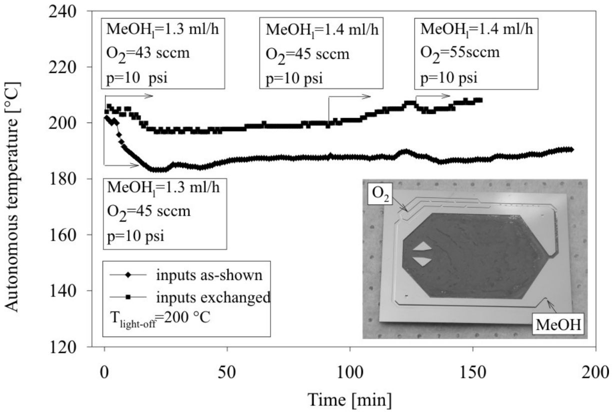

Figure 10: Autonomous combustor temperature with separate oxygen and methanol inputs and internal mixing on the platform for two modes of reagent supply.

In certain cases the generated heat was insufficient to rise the temperature and the output contained some unreacted methanol in particularly when the reaction was under fuel rich conditions or the mixing was insufficient. The residence time of MeOH-air/oxygen mixture in the cavity has to be longer than the time required for the chemical reaction. This is described by a Damkohler number and should be >1. It is assumed that in certain cases this condition was not fulfilled. On the other hand, excessive amounts of input methanol cause that the catalyst is no longer capable of proper function and simultaneously, the unreacted components are expelled to the outside ambient by the pressure difference. The reactor could even become flooded with liquid methanol if the evaporation is not fully completed.

It was also observed that when a certain oxygen flow rate is exceeded, the methanol pressure from the syringe pump was actually insufficient for introduction into the microchannel due to oxygen pressure interference. This was the limitation for increasing further the methanol feed. Therefore, at this point we were just able to maintain the reaction and the temperature, but could not increase it by increasing the feed rate. Limitations for achieving autonomous combustion can be found in specific geometry of the chamber, efficiency of mixing unit, exhaust orifice size, co-dependency of inlet pressures of both reagents and the reaction type taking place (heterogeneous only or transition toward homogeneous).

Table 1 and 2 shows conditions corresponding to two input configurations also presented in Fig. 10, indicating successful self-sustaining combusting parameters and the output products.

Table 1: Combustor input conditions and output products in separate feed mode-standard input ports.

MeOH [ml/h]	O2 [sccm]	H2O [µg/min]	H2O+MeOH	autonomy
1	35	6,7		no
1,2	43		11,8	no
1,3	45	13,8		yes

Table 2: Combustor input conditions and output products in separate feed mode-exchanged input ports.

MeOH [ml/h]	O2 [sccm]	H2O [µg/min]	H2O+MeOH	autonomy
1	35	10,5		no
1,2	35		13,21	no
1,2	43	13,5		no
1,3	43	15,05		no
1,3	43	16,16		yes
1,4	45	17,3		yes

Characterization of combustor with premixed MeOH + O2/air fuel

For this mode of fuel delivery, bubbler principle was used to feed the microcombustor, which was mounted into the SS housing and insulated by rock wool. As shown schematically in Fig. 4c, oxygen or air stream carrier gas enters the liquid methanol vessel and bubbles rise through the methanol into the vapor phase above where it is further mixed with saturated methanol vapors and then exit into the feeding line toward reactor. When it reaches the catalyst covered chamber, the reaction (eq.1) takes place after the proper ignition conditions are met such as light-off temperature, sufficient catalyst activity and fuel to oxygen ratio.

Combustor temperature vs. partial pressure of methanol and carrier gas flow rate

The bubbler temperature determines the partial pressure of saturated methanol vapors and must be well controlled. If the volume above the methanol liquid level is saturated, the inlet oxygen or air flow mixes with methanol vapors and transports it toward the outlet, thus depleting the methanol concentration in the bubbler. Dynamic process of forming the vapor phase above the surface of the liquid methanol has to maintain equilibrium with the carrier gas at certain temperature. Carrier gas has actually two functions, i.e. promotes the mass transport of methanol vapors into the combusting cavity and also takes a part in the combusting reaction, and therefore has to be carefully adjusted to meet both requirements.

As discussed also by Ma et al. [14], when the carrier gas velocity increases (i.e. inlet flow rate is increased), methanol concentration slightly decreases (i.e. ratio F=Fuel/Air, decreases), indicating that the residence time in bubbler is increasingly too short for the air to fully saturate with methanol at higher flow rates.

At a constant flow of carrier gas through the bubbler, the quantity of methanol vapor entering the combustor is increased by the temperature of bubbler and so is the temperature of the combustor (Fig. 11). Therefore also carrier gas amount has to be sufficient to fulfill the stoichiometric ratio for the reaction or to be slightly above it (fuel lean conditions). By this means the entire methanol will be reacted (oxidized) and no unreacted methanol will appear at the exit of combustor. In this case only water and CO_2 will be the byproduct. This is actually a good indicator of complete reaction taking place in the cavity. If we obtain the unreacted (surplus) methanol at the exit, this indicates the reaction was not complete due to mixture ratio or geometrical and catalyst efficiency limitations for the overall quantity of input energent, as discussed also in previous section.

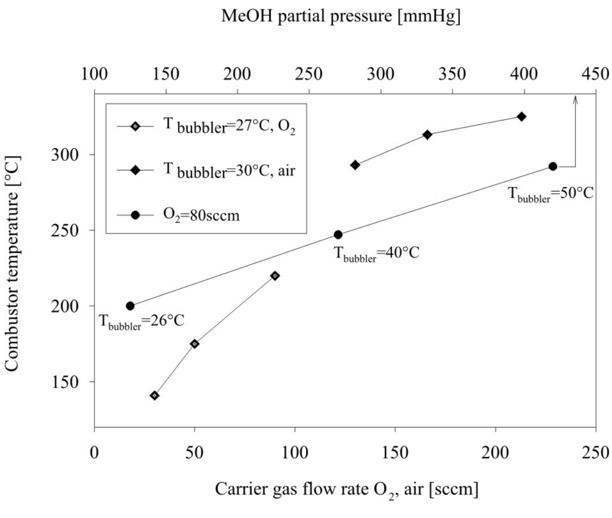

Figure 11: Dependency of methanol partial pressure (bubbler temperature) and carrier gas flow rate on the combustor temperature.

As shown in Fig. 11, adjusting the combustor temperature can be performed by controlling partial pressure of methanol vapor or by adjusting the carrier gas flow rate within the reasonable range, limited by the combustor design and thermodynamic issues such as residence time or reaction mode. Fig. 12 shows the heat up curve of the combustor in autonomous regime, followed by instant combustor response to reduced carrier gas flow rate and steady state temperature that could be obtained after prolonged period. The transient is rather long (>100 min) due to the high thermal load of the combustor housing. For oxygen as a carrier gas, the combusting efficiency of 85-90% was determined by measuring the amount of output water from the combusting process, with respect to calculated stoichiometric water product. The combusting efficiency with air was determined to be 80-85 %, which is slightly lower compared to oxygen carrier gas.

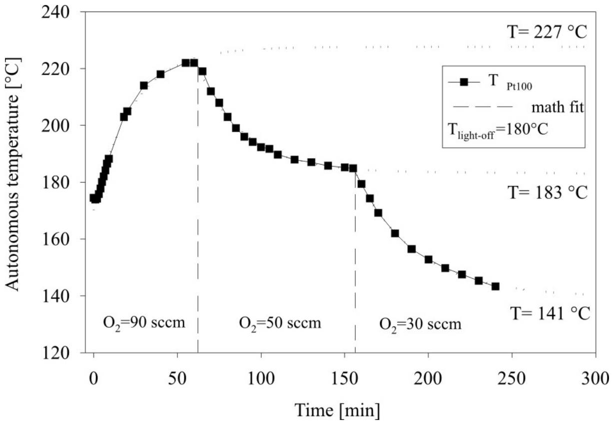

Figure 12: Influence of oxygen flow rate on the combustor temperature in autonomous regime.

Fig.13 presents the influence of the some additional insulation details on the obtained final temperature of the combustor when fed with constant amount of input fuel. For the given input parameters, the temperature reached was 280 °C when the combustor was insulated by 20 mm thick rock wool shield. During experiments, the exhaust hood was mounted above the reactor due to safety reasons if unreacted methanol exits. This causes forced convection around the combustor. When it was removed, the temperature slightly increases up to 286 °C. By lifting the rock wool insulated combustor from the table and putting it on the three small posts (decreasing thus the conductive heat losses) additional slight increase of temperature was obtained. To further reduce heat losses caused by radiation, the system was enclosed with Al foil and the temperature was increased to 293 °C. All three steps cumulatively contributed to rise of temperature (e.g. 13 °C or 4.6%). The insulation issues need to be considered further in order to reduce heat losses and achieve faster thermal response. Though it is desirable to have fast thermal response of the system, this also means that the system will be sensitive to undesired ambient changes. As shown in Fig.13, the consumption of liquid methanol during 6 hours period was as low as 1.1 ml/h to maintain the combustor temperature between 280 and 293 °C.

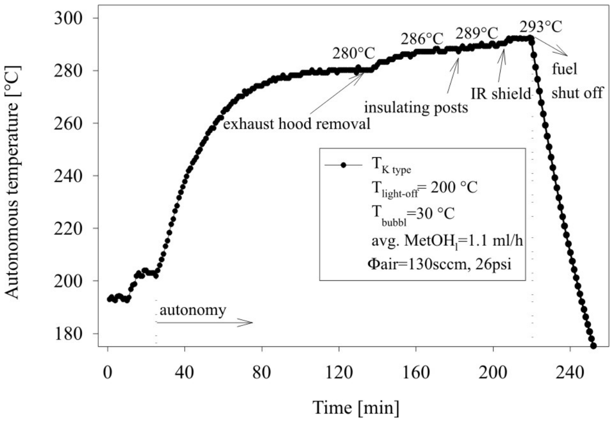

Figure 13: Influence of additional insulating steps on the steady state temperature of combustor.

In the case of air carrier gas, the reaction reagents are diluted by additional nitrogen. Equilibrium between the introduction of methanol vapors and needed oxygen from the air carrier gas has to be established. The outgoing products contain also inert N_2 carrier gas. If the flow rate of air is too high, the amount of unreacted methanol over the catalyst can exceed the ability of catalyst to support the reaction (residence time is too short) and some methanol can leave the combustor unreacted.

The influence of light-off temperature in the range 80-200 °C on temperature rise time was studied in more details in a previous work [16]. It was shown that the combustion was successful for light-off temperature of 100 °C and above. At 80 °C, the ignition level was too low and the reaction did not take place at all. By providing higher light-off temperatures and implementing oxygen carrier gas instead of air, the transition of heterogeneous type of reaction to self-sustained homogeneous was found to decrease.

Fig. 14a presents SEM top view of mesoporous ceria and nanodispersed Pt and Fig. 14b presents cross-section of catalyst layer on the Si substrate. The catalyst layer was examined after performing several experiments (cumulatively >100 h) under different feed conditions. No changes in morphology or carbonaceous deposits were found on the catalyst layer, indicating that the catalyst layer can withstand severe overloading or fuel rich conditions.

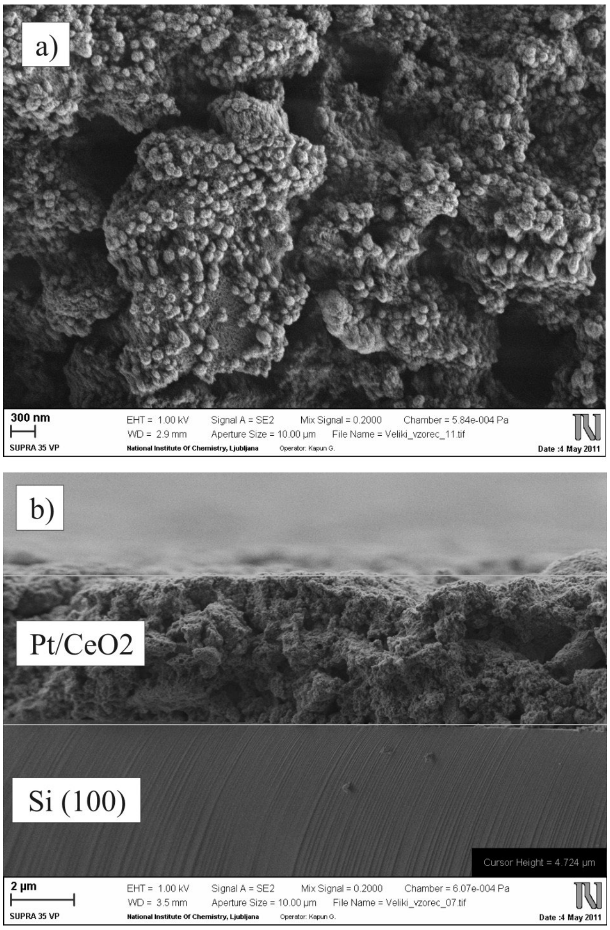

Figure 14: Deposited Pt/CeO_2 catalyst within the combustor chamber: a) top view and b) cross section.

Discussion on the presented combusting approaches:

Each of the presented approaches in this study offer certain advantages and disadvantages. The applicability of individual approach depends strongly on the field of application, type of available or required energent, light-off temperature, range of aimed working temperature and similar. Table 3 summarizes some results obtained during this study. Due to the fact that parameters for each approach were different the data given correspond only to given process conditions and type of combustor design.

Though the advantageous self-ignition can be obtained already at RT as shown in Fig. 5, H_2-O_2 energent is eventually not a practical type of fuel for portable applications, because it is not widely available in field operations, nor as a separate storage tanks neither from anode of fuel cell as the excessive hydrogen. For fast start up from RT, all three presented approaches actually require additional energy, usually heating by e.g. thin film Pt electrical heaters [19]. More efficient temperature time response at RT light-off could eliminate need for electrical heating.

As shown in the table 3, combustor with in-situ mixing showed relatively good efficiency, however the fuel evaporation and mixing realized on the same Si platform is a rather demanding task. There is a strong interplay between geometrical issues, evaporation paths, mixing efficiency as well as precise control of the amount and ratio of mixed fuel reaching the catalyst surface [20]. The consequence is that combustion process and final temperature are not easy to control independently. Further work is still required to optimize the combustor design for higher performance. Important fact that was determined by our experimental work was that certain combustor design covers only a limited range of working parameters where optimal efficiency is obtained; once out of range, the ignition is not reached or the oxidation process is not completed (unreacted products are detected) or the combustion is completely ceased.

Our experimental results show that for the type of designed reactors, the most suitable methanol feed approach is by premixing air or oxygen and methanol via bubbler. It was shown that final temperature can be well controlled with adjusting the input parameters and by proper heat loss management. From the point of repeatability, combusting of premixed MeOH-O_2/air showed superior results compared to H_2-O_2 or in-situ mixing.

Long-term stability tests with bubbler type autonomous combusting over prolonged period also revealed the best performance as shown in our previous work [16]. In that study the measured average consumption rate of liquid methanol to maintain 320 °C temperature over 7 hour period was below 1.45 ml h^{-1} and the stability 320 ±1 °C. Taking into account the determined combusting efficiency of 90%, the delivered average thermal power in that case was 6.5W [16]. Unfortunately, bubbler type of dosing is not practical in the field due to drawbacks such as required tight control of bubbler temperature and being also position sensitive. The solution of internal mixing is still preferred for field operation, therefore abovementioned problems require further attention.

4. Conclusions

Design, microfabrication process and characterization of silicon-glass based microcombustor with Pt/CeO_2 catalyst, as a heat provider for various endothermic processes, were presented. The influence of some important parameters, such as input flow rate of reagents, premixing regime, pressure and light-off temperature were presented and discussed. Three different types of fuel application were presented and each characterized by means of thermal response characteristics and heat provisions. The prepared Pt/CeO_2 catalyst proved very efficient, providing the ignition of H_2-O_2 energents already at room temperature. Bubbler type of methanol air/oxygen fuel delivery exhibited the most promising results regarding the provided heat, temperature control and methanol consumption. This type of microcombustor exhibited average consumption rate of liquid methanol typically 1.1 ml h^{-1} to maintain temperature 290 ±1 °C °C.

Acknowledgments

This work was supported by the Ministry of Defense of the Republic of Slovenia (Grant No. MORS 345/2007-RR) and Slovene Research Agency (No. P2-0152). The authors would like to extend their gratitude to dr. J. Batista from National Institute of Chemistry, Slovenia, for catalyst preparation.

References

1. A.M. Karim, J.A. Federici, D.G. Vlachos, Portable power production from methanol in an integrated thermoelectric/microreactor system, J. Power Sources 179 (2008) 113-120.

Table 3: Summarized performances at specific parameters for the presented combusting approaches.

Energent type	Light-off temperature [°C]	Efficiency %	Final temperature [°C]	Fuel consumption
H2-O2	100	63	210	40/20 sccm
MeOH+O2 (pre-mixed)	180	89	225	0.9 ml/min MeOH 90 sccm O2
MeOH+air (pre-mixed)	160	84	293	1.1ml/h MeOH 130sccm air
MeOH+O2 (in-situ mix)	200	86	200	1.3ml/h MeOH 43sccm O2

2. J.D. Morse, Micro-fuel cell power sources, Int. J. Energy Res. 31 (2007) 576–602.
3. K. Shah, R.S. Besser, Key issues in the microchemical systems-based methanol fuel processor: Energy density, thermal integration, and heat loss mechanisms, J. Power Sources 166 (2007) 177-193.
4. B. Lindström, L.J. Pettersson, Catalytic oxidation of liquid methanol as a heat source for an automotive reformer, Chem. Eng. Technol. 26 (2003) 473-478.
5. J.F. Pan, W.M. Yang, A.K. Tang, S.K. Chou, L. Duan, X.C. Li, H. Xue, Micro combustor in sub-millimeter channels for novel modular thermophotovoltaic power generators, J. Micromech. Microeng. 20 (2010) 125021 (8pp).
6. J.A. Federici, D.G. Norton, T. Brüggemann, K.W. Voit, E.D. Wetzel, D.G. Vlachos, Catalytic micro combustors with integrated thermoelectric elements for portable power production, J. Power Sources 161 (2006) 1469-1478.
7. J. Y. Won, H. K. Yun, M. K. Yeon, S. I. Woo, Performance of micro channel reactor combined with combustor for methanol reforming, Catal. Today 111 (2006) 158-163.
8. S.-K. Ryi, J.-S. Park, S.-H. Choi, S.-H. Cho, S.-H. Kim, Novel micro fuel processor for PEMFCs with heat generation by catalytic combustion, Chem. Eng. J., 113, (2005), 47-53.
9. K. Yoshida, S. Tanaka, H. Hiraki, M. Esashi, A micro fuel reformer integrated with a combustor and a micro channel evaporator, J. Micromech. Microeng. 16 (2006) S 191-197.
10. J.D. Morse, R.S. Upadhye, R.T. Graff, C. Spadaccini, H.G. Park, E.K. Hart, A MEMS-based reformed methanol fuel cell for portable power, J. Micromech. Microeng. 17 (2007) S237-S242.
11. G.-G. Park, S.-D. Yim, Y.-G. Yoon, C.-S. Kim, D.-J. Seo, K. Eguchi, Hydrogen production with integrated micro channel fuel processor using methanol for portable fuel cell systems, Catal. Today 110 (2005) 108-113.
12. D.-E. Park, T. Kim, S. Kwon, C.-K. Kim, E. Yoon, Micromachined methanol steam reforming system as a hydrogen supplier for portable proton exchange membrane fuel cells, Sens. Actuators A 135 (2007) 58-66.
13. Z. Hu, V. Boiadjiev, T. Thundat, Nanocatalytic spontaneous ignition and self-supporting room-temperature combustion, Energ. Fuel. 19 (2005) 855-858.
14. Y. Ma, C. Ricciuti, T. Miller, J. Kadlowec, H. Pearlman, Enhanced catalytic combustion using sub-micrometer and nano-size platinum particles, Energ. Fuel. 22 (2008) 3695-3700.
15. P. Djinović, J. Batista, J. Levec, A. Pintar, Comparison of water–gas shift reaction activity and long-term stability of nanostructured CuO-CeO_2 catalysts prepared by hard template and co-precipitation methods, Appl. Catal. A 364 (2009) 156-165.
16. D. Resnik, S. Hočevar, J. Batista, D. Vrtačnik, M. Možek, S. Amon, Si based methanol micro combustor for integrated steam reformer applications Sens. Actuators A (2012).
17. A.A.S. Bhagat, E.T.K. Peterson, I. Papautsky, A passive planar micromixer with obstructions for mixing at low Reynolds numbers, J. Micromech. Microeng. 17 (2007) 1017-1024.
18. H. Wu, M. Yu, P. Cheng, X. Wu, Injection flow during steam condensation in silicon microchannels, J. Micromech. Microeng. 17 (2007) 1618-1627.
19. D. Resnik, D. Vrtačnik, M. Možek, B. Pečar, S. Amon, Experimental study of heat-treated thin film Ti/Pt heater and temperature sensor properties on a Si microfluidic platform, J. Micromech. Microeng. 21 (2011) 025025 (10pp).
20. B. Pečar, M. Možek, D. Resnik, D. Vrtačnik, U. Aljančič, S. Penič, S. Amon, Microflow generator for fuel cell methanol hydrogen microreactor, Informacije MIDEM = Journal of microelectronics, electronic components and materials ISSN: 0352-9045.- Letn. 40, št. 3 (sep. 2010), str. 208-217.

Arrived: 17. 08. 2012
Accepted: 5. 11. 2012